Contents lists available at Growing Science

Current Chemistry Letters

homepage: www.GrowingScience.com/ccl

Biological evaluation of inhibitors of reverse transcriptase from HIV type-1

Hitendra Kumar Lautre[a*], Taibi Ben Hadda[b], Snigdha Das[c] and Ajai Kumar Pillai[a]

[a]*Department of Chemistry, Govt.V.Y.T.P.G.Autonomous College, Durg (C.G.) India, 491001*
[b]*Material Chemistry Laboratories, FSO, Mohammed First University, Oujda 60000, Morocco*
[c]*Sachdeva International School, Dhusera, Raipur (C.G.) India, 492001*

C H R O N I C L E

Article history:
Received October 21, 2014
Received in revised form
December 02, 2014
Accepted 12 December 2014
Available online
12 December 2014

Keywords:
N-hydroxy-4-[(hydroxyimino)methyl]benzamidine
Reverse transcriptase inhibitor
HIV-1
Metal complexes
Antibacterial activity

A B S T R A C T

In the present work, Zn(II), Co(II) and Cr(II) metal complexes **(3-5)** of N-hydroxy-4-[(hydroxyimino)methyl]benzamidine ligand **(2)** were synthesized and their anti-HIV activity by inhibiting reverse transcriptase was explored. Structural characterization using NMR, FTIR, Mass, UV-Vis spectra, TGA, magnetic moment and elemental analyses were performed. The analyses show that geometry, lipophilicity and steric factor play crucial role. Cell viability test is performed on peripheral blood mononuclear cells to check toxicity of prepared compounds on immune system, shows toxicity only at higher concentration. Antimicrobial activity and DNA cleavage analysis have also been studied and reported.

1. Introduction

Human Immunodeficiency Virus (HIV) is a retrovirus of lentivirus family and contains a reverse transcriptase (RT) enzyme responsible for making a DNA copy of the viral RNA. This virus attacks human cell and attach to CD4 and chemokine receptors on the membrane and release RNA to the cytoplasm. Reverse transcriptase catalyzes this process and help in DNA synthesis. Thus RT plays a crucial role in virus survival and cell progression. Intensive studies of this enzyme by researchers have attracted our interest to inhibit proliferation of HIV cell. Wide variety of drugs has been developed for HIV based on these studies is available in market. These HIV-1 drugs are divided in nucleoside (NRTIs, AZT, e.g., 3TC, and ddC) and non-nucleoside (NNRTIs e.g., nevirapine, delaviridine) reverse transcriptase inhibitors[1-5]. Non-nucleoside inhibitors are most widely used for the treatment of HIV-1-infection[6].

* Corresponding author. Tel: 00918982431911
E-mail address: lautre.hitendra@gmail.com (H.K. Lautre)

doi: 10.5267/j.ccl.2014.12.002

The rapid development of resistance to these available drugs by HIV cell has diminished the effectiveness of current approved NNRTIs in the market, leading to urgent need of next generation NNRTIs. Large number of computation methods have been reported to find new drug candidate, this are based on Quantitative structure–activity relationship (QSAR) techniques. This technique correlates biological activity to their physicochemical properties[7].

It is necessary to study the accurate physicochemical and biological properties using QSAR techniques. QSAR data obtained from various research works confirm the docking of NNRTIs to a specific allosteric non-substrate binding pocket site (Non-nucleoside binding pocket-NNBP[8]. A number of Pharmacophore modeling studies have been performed to find out the better inhibitor of RT. It helps medicinal chemist to filter out the active ingredients before synthesis. Various properties of drug affect their activity like solubility, hydrophobicity, PSA (Polar Surface Area), and steric factor. *In silico* studies by various computer applications help in determining this parameter using virtual screening[9,10]. QSAR studies on metal compounds have also been probed for potential anti-HIV therapeutic actions. Some study reports metal based anti-viral compounds like, ruthenium complex Na_7-[Ru_4(l-O)$_4$(C_2O_4)$_6$], eilatin ruthenium complexes, and oxovanadium(IV) porphyrin complexes possess anti-HIV-1 activity[11,13].

A study on Gold cyanide, $[Au(CN)_2]^-$ complex was reported as anti-HIV agent acting by inhibiting RT[14]. A wide variety of amidine compounds have been found to be active against viral, fungal and bacterial diseases. Amidine are the Schiff base derivatives have wide variety of biological activities thus used in viral fungal and bacterial disease[15]. Some metal complexes of amidine have been synthesized and evaluated their antimicrobial and antitumoral activity[16,17]. In order to gain further insights, we have carried out *in vitro* inhibition of reverse transcriptase (RT) enzyme from HIV cell. The present article describe the synthesis of Zn(II), Cr(II) and Co(II) complexes **(3-5)** of N-hydroxy-4-[(hydroxyimino)methyl]benzamidine **(2)** biological evaluation as reverse transcriptase inhibitors from HIV type-1.

2. Results and Discussion

2.1. Spectral studies

2.1.1. ^{1}H NMR spectral studies

^{1}H NMR spectra of ligand **(2)** displayed distal hydroxyl proton H-14 peak at 10.93 ppm and H-2, H-6, H-5 and H-1 protons of benzene ring at 7.39-7.47 ppm as doublet of doublet. Distal H-12 (free hydrogen) proton appeared at 7.82 ppm as singlet, confirming the structure of ligand **(2)** (**Figure 1**). A singlet was observed at 5.99 ppm assigned for (C=NH) protons of hydroxyamidine moiety. Peak at 9.88 ppm was assigned for (=N-OH) proton. As the formation of metal complexes many changes were observed in the chemical shifts, it was confirmed by the disappearance of amidine hydroxyl (-OH) proton. In all metal complexes of Zn(II), Co(II) and Cr(II), (Ar-CH_3) protons remains its position. A singlet of (=C-NH_2) proton was observed lower downfield at 1.50 ppm than ligand (2). H-11, H-12, H-14 and H-15 showed multiplate between 7.90-7.97 ppm of aromatic ring (**Figure 1**). Distal proton was observed at 8.07 and 8.29 ppm. A singlet was observed for distal hydroxyl group H-24 at 10.93 ppm. Distal (N-OH) was observed at 10.91 and 10.93 ppm for Zn(II) and Co(II) complex respectively. Similarly (H-C=N) was showed at 8.29 and 8.25 ppm for Cr(II) and Zn(II) complex. Furthermore, the number of the proton calculated from the integration curves and those obtained from the values of the expected CHN analysis agreed well with each other.

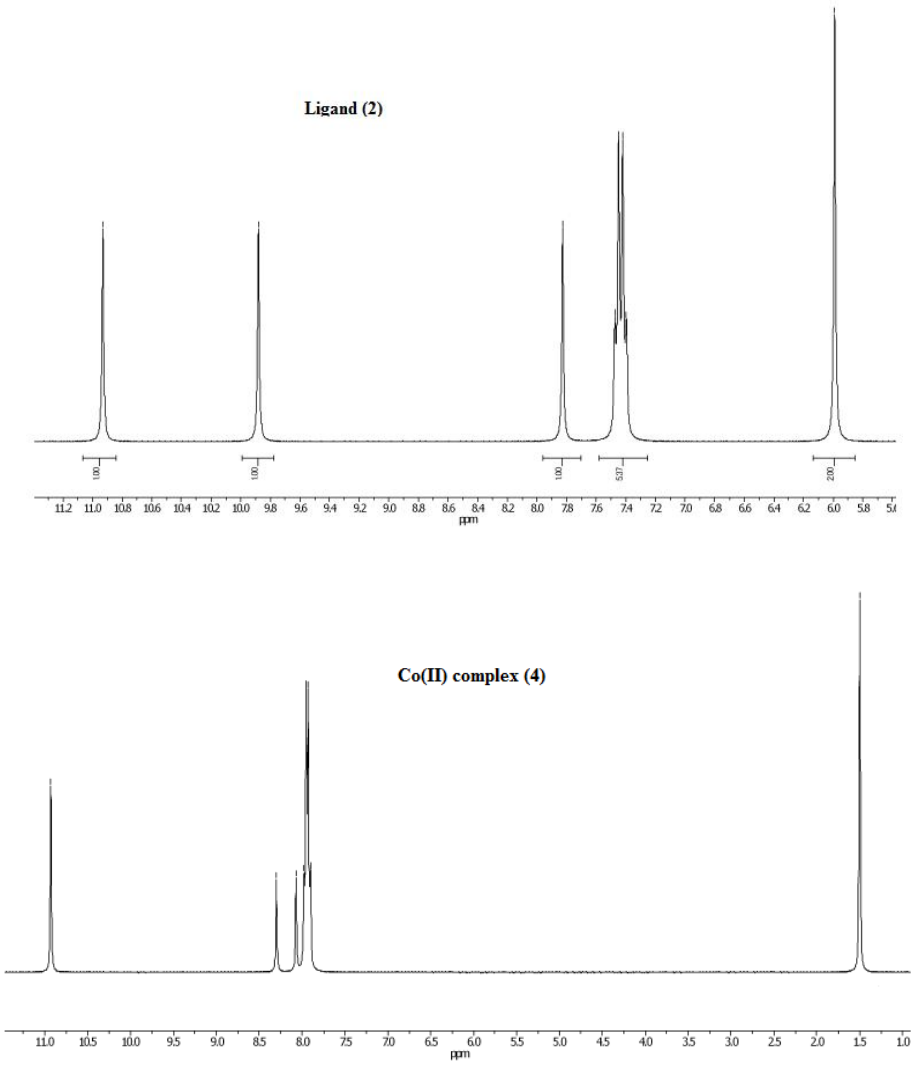

Fig. 1. ^{1}H NMR spectra of HIMB ligand (**2**) and its Co(II) complex (**4**).

2.1.2.^{13}C NMR spectral studies

^{13}C NMR spectra of ligand **(2)** displayed the entire characteristic peak at the expected position which further supported the results obtained in IR and ^{1}H NMR. The C2 and C6 carbons of ligand **(2)** containing showed shift at 130.24 ppm, similarly C1 and C5 carbon gives shifting peak downward at 128.78 ppm, due to the sharing of electron of nitrogen towards the benzene ring system. Amidine moiety containing C7 were assigned at more downfield 153.10 ppm due to deshielding effect. Another characteristic peak of distal C11 was observed at 149.34 ppm. As the complexes were formed many changes in chemical shifting were found. Amandine carbon C5 and C8 were shifted to some higher downfield at 149.34 ppm than ligand **(2)** due to increase in electron cloud and hence hindrance. Ring carbon C18 and C10 attached to amidine moiety (C5 and C8) showed only a slight shifting at position 129.60 ppm, due to increase in electron cloud on metal coordination. Aromatic carbon C13, C14 and C12 attached to iminomethyl group was observed at 130.74 ppm, and the carbon C27 of iminomethyl group at 149.34 ppm. Other carbon in amidine moiety was observed at 152.99 ppm. Furthermore, the number of carbons calculated from the integration curve and those obtained from the values of the expected CHN analyses agree well with each other.

2.1.3. IR spectral investigations

The IR spectra of the complexes have been examined in comparison with the spectra of the N-hydroxy-4-[(hydroxyimino)methyl]benzamidine ligand **(2)**. IR spectra of the ligand **(2)** in particular show main characteristic absorptions in the range 1653, 972, 2914, 3495 and 3292 cm^{-1}, which can be assigned to C=N, NO, C-N, distal OH and amidine OH stretching vibrations, respectively.

Table 1. IR frequencies of HIMB ligand (**2**) and its metal complexes (**3-5**)

Compounds	IR frequencies (cm^{-1})					
	C=N	N-O	C-N	O-H	M-O	M-N
Ligand (2)	1653	972	2914	3292	-	-
HIMBZn (3)	1660	1024	2871	-	543	511
HIMBCo (4)	1648	993	2700	-	520	570
HIMBCr (5)	1665	1010	2710	-	530	580

All the other functional group vibrations are appeared at their expected positions. **Table 1** show the characteristic peak for distal OH group in ligand **(2)**, appeared at 3495 cm^{-1}, which on coordination to metal ion shifted in the range 3010-3344 cm^{-1} as a broad peak. On coordination of Zn(II), Cr(II) and Co(II) metal ion with ligand **(2)**, (amidine, OH) frequency disappeared and new MO bond formed showed stretching frequencies 543, 530 and 520 cm^{-1} respectively. Metal(II) ion also coordinate with (NH_2) giving transmittance between 511-580 cm^{-1}. The (C=N) bond also showed stretching frequencies higher in Co(II) complex of value 1648 cm^{-1}, as compared to ligand **(2)** (1660 cm^{-1}) and other complexes. The (NH_2) group attached to benzene ring showed chemical shift of 2914, 2871, 2710 and 2700 cm^{-1} for ligand **(2)**, Zn(II), Cr(II) and Co(II) complexes respectively. Other peaks were observed at their respective positions.

2.1.4. Electronic spectra and magnetic moments

The UV absorption spectra of ligand **(2)** and its complexes at very low concentrations are recorded in the wavelength range 200–700 nm using a VARIAN UV–Vis spectrophotometer. It was seen that ligand **(2)** display peaks at around 260 nm, corresponding to π- π* transition due to phenyl ring. Another characteristic peak at 350 nm was observed due to n-π* transition of C=N group. As the complex formed many changes were seen. In the Zn(II) complex blue shift were seen, the higher energy spectra of the complex was shown at 250 and 310 nm correspond to the ligand **(2)** π- π* transition and ligand **(2)** to metal charge transfer π- π* transition.

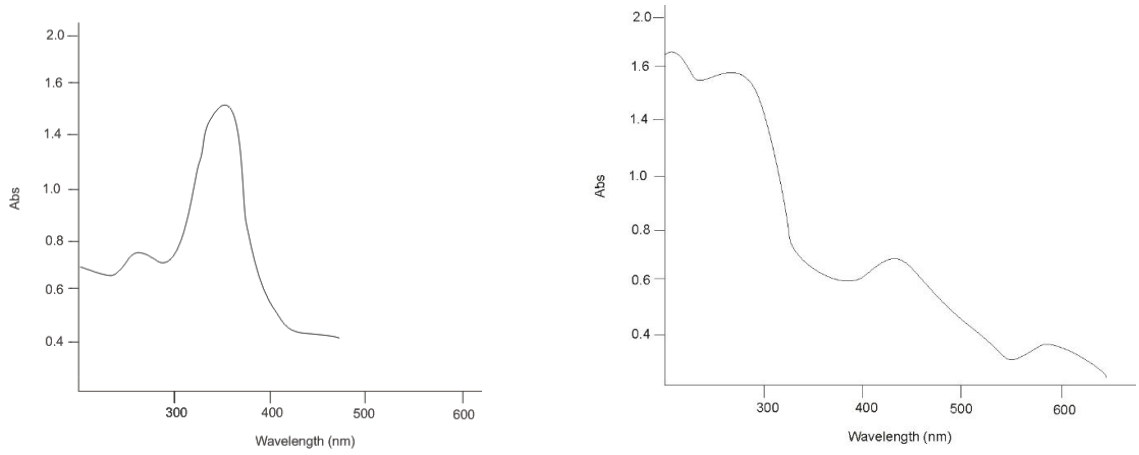

Ligand **(2)** Cr(II) complex **(5)**

Fig. 2. UV-Vis spectra of HIMB ligand **(2)** and their Cr(II) complex **(5)**

A low energy spectrum was observed at 420 nm and maximum wavelength due to ligand **(2)** to metal charge transfer. The electronic spectra of Cr(II) and Co(II) complexes were also studied and found many peaks correspond to various transitions. The absorption peak at 240 and 210 nm due to ligand (2) π- π* transition in Co(II) and Cr(II) complexes respectively in the UV region **(Figure 2)**. An n-π* transition was confirmed by the absorption peak at 280-300 nm correspond to C=N, which shifted towards the lower wavelength and higher energy on coordination with metal ions. Magnetic moment of Co(II) complex was observed 1.7 BM which is characteristic of low spin d^7 ions in octahedral field. The ligand **(2)** to metal charge transfer was observed at 500 nm in Co(II) complex and 420 nm in Cr(II) complex a low energy d-d transition was observed at 600 nm (high energy) and 580 nm (low energy) in Co(II) and Cr(II) complex respectively, confirming there octahedral geometry. The magnetic moment observed for Cr(II) complex is quite low (2.9 BM) for d^4 ions in octahedral field. This value could be caused by significant distortion from ideal geometry, which leads to a fall in the orbital contribution to the magnetic moment.

2.1.5. Mass spectral studies

The mass spectral characterization of N-hydroxy-4-[(hydroxyimino)methyl]benzamidine and its Zn(II), Cr(II) and Co(II) complexes were performed to confirm their orientation. The molecular ion peak at m/z 179.10, 444.32, 451.29 and 421.74 corresponds to ligand **(2)**, Cr(II), Co(II) and Zn(II) complexes related to their molecular weight. The peak at 163.17, 404.74, 398.26 and 391.33 corresponds to the isotopic abundance after removal of distal hydroxyl group. Phenyl ring was removed and the peak was observed at 253.12 and 177.02 in Zn(II) complex and 259.59, 246.8 and 170.09 in Cr(II) and Co(II) complexes. The water molecule was removed and the corresponding peak was observed at 433.2 and 415.26 for Co(II) complex, 426.34 and 408.33 for Cr(II) complex. The removal of coordinated water molecule in both these complexes confirms there octahedral geometry.

2.2. Thermo gravimetric analysis (TGA)

The thermal properties of the ligand **(2)** and its metal complexes were investigated by thermal gravimetric analysis (TGA). **Fig. 3** shows the recorded curve of N-hydroxy-4-[(hydroxyimino)methyl]benzamidine and their Zn(II), Co(II) and Cr(II) complexes under nitrogen atmosphere with a heating rate of 10°C/min at temperature range 20-1000°C. The analysis shows that all the compounds except ligand **(2)** are thermally stable. It was seen that ligand **(2)** start decomposing at 93°C, 50% decomposition was observed in these range. Other 30% decomposition was observed between 93-600°C. The Co(II) and Cr(II) complexes were decomposed at 210 and 240°C respectively. TGA curve display 30% decomposition of Co(II) complex in the range 250-350°C and Cr(II) complex in the range 240-400 of 30%. Remaining 40% decomposition was observed in the range 390-600°C for Cr(II) complex and 50% decomposition in the range 350-690°C for Cr(II) complex. TGA curve showed decomposition of Zn(II) complex in two steps, first was observed at 180-530°C of about 52%. Second step involve with the decomposition of 25% in the range 530-600.

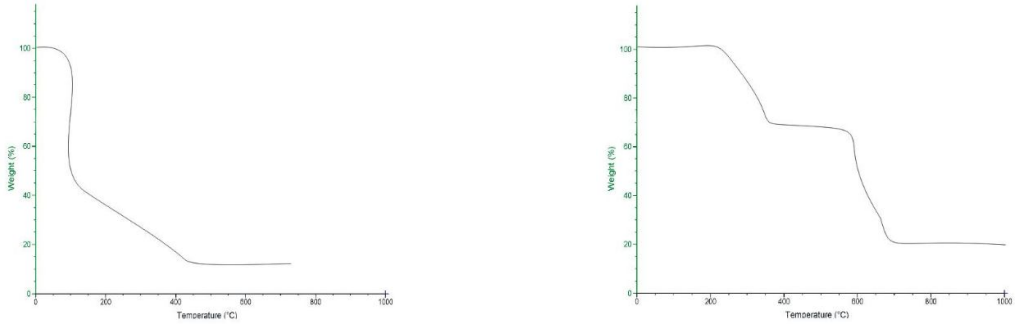

HIMB ligand **(2)** Co(II) complex

Fig. 3. TGA curve of HIMB ligand **(2)** and its Cr(II) complex

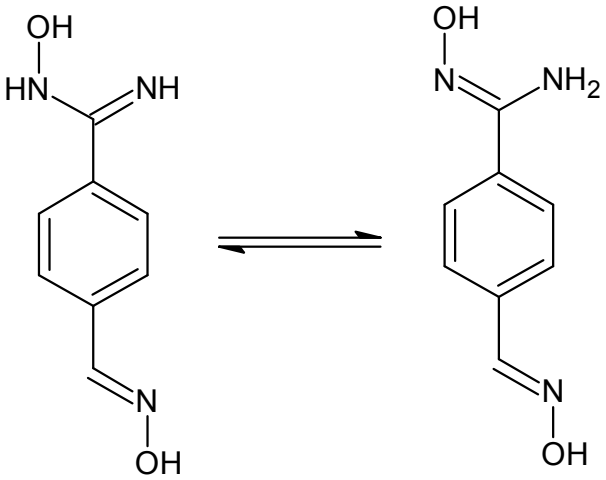

Fig. 4. Tautomerization of N-hydroxy-4-[(hydroxyimino)methyl]benzamidine.

2.2. Biological study

2.2.1. DNA cleavage study

DNA cleavage activity of prepared compounds was analyzed by monitoring the conversion of supercoiled DNA (Form I) to nicked DNA (Form II) and linear DNA (Form III) under anaerobic conditions. No DNA cleavage was found for the lane 1 and Lane 2 which incorporates with the DNA control and (DNA + H_2O_2) respectively (**Fig. 5**). It was observed that ligand **(2)** at 70 μM concentration can induce almost 80% supercoiled DNA to linear and nicked DNA (lane 3). It was observed that Cr(II) and Co(II) complexes can almost promote 65% cleavage at their maximum concentration of 50 μM. At lower concentration no cleavage was observed for these complexes. No significant conversion of CTDNA was observed for Zn(II) complex up to their maximum concentration of 50 μM.

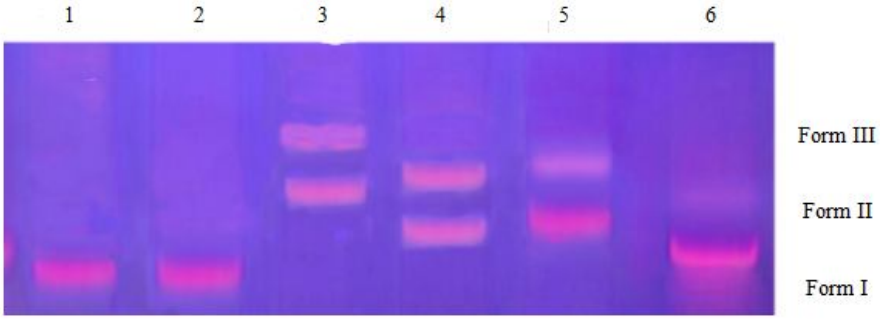

Fig. 5. Gel electrophoresis diagram showing the cleavage of CT DNA by Cr(II),Zn(II) and Co(II) complexes in a buffer containing 50 μM Tris–HCl and 50 μM NaCl in the presence of H_2O_2 at 37 ◦C. Lane 1, DNA control; lane 2, DNA + H_2O_2; lane 3, DNA + ligand (2)(L)] + H_2O_2; lane 4, DNA + H_2O_2 + [CrL]; lane 5, DNA + H_2O_2 + [CoL] and lane 6, DNA + H_2O_2 + [ZnL].

2.2.2. Antifungal activity

The antifungal activities of all compounds were tested against *T.longifusus*, *C.albican*, *A.flavus* and *P.carinii* fungal strain. It was observed that Cr(II) and Co(II) complexes showed significant activity against *T.longifusus* (MIC- 75 μM/ml). All the compounds were active against *C.albican* except Zn(II) complex, but Co(II) showed good activity (MIC- 208 μM/ml). The Cr(II) complex was not active against (**Table 2, Fig. 6**), highest activity was observed for Co(II) complex (MIC- 100 μM/ml). Only

Zn(II) and Co(II) complexes showed activity against *A.flavus*, but Co(II) complex was showed significant activity (MIC- 50 µM/ml). All the compounds showed weak to moderate activity against *P.carinii*, but ligand **(2)** showed significant activity (MIC- 90 µM/ml) compared to those of standard drug miconazole (**Table 3**). Two tautomeric analogues of HIMB ligand **(2)** are proposed which is responsible for antimicrobial activity. Thus the charge is distributed; it could generate the in situ presence of antibacterial and antifungal activity (**Fig. 4**).

Table 2. Minimum inhibitory concentration of HIMB ligand **(2)** and its metal ion complexes against selected fungal species

Code	Compounds	Minimum inhibitory concentration (in µM)			
		T.longifusus	*C.albican*	*A.flavus*	*P.carinii*
2	HIMB	208	210	--	90
3	HIMBZn	--	350	170	300
4	HIMBCo	70	100	50	400
5	HIMBCr	75	--	--	455
SD	Miconazole	110	135	68	130

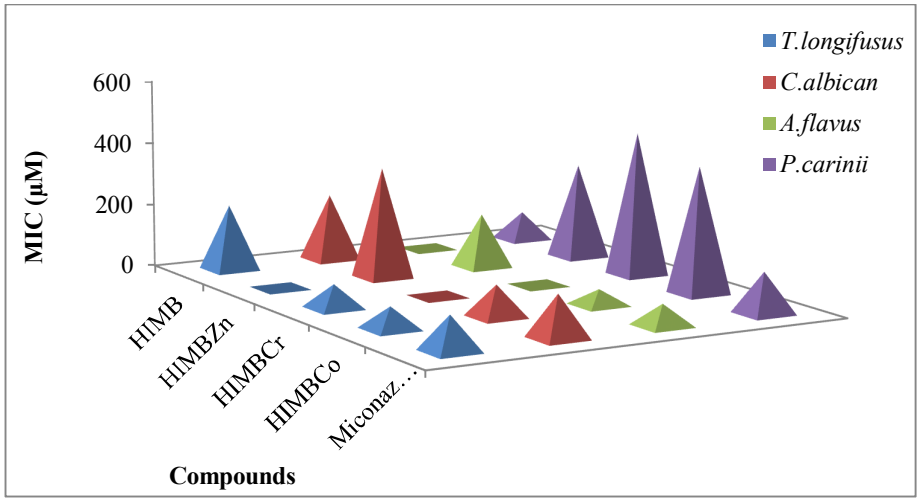

Fig. 6. Minimum inhibitory concentration of HIMB ligand **(2)** and their metal ion complexes against selected fungal species

2.2.3. Antibacterial activity

The N-hydroxy-4-[(hydroxyimino)methyl]benzamidine and their metal ion complexes were synthesized, characterized and their antibacterial activity were studied against four selected bacterial strain *B.subtilis*, *S.aureus*, *B.cereus* and *S.pneumoniae*. All the compounds showed varying degree of inhibitory activity against selected species. All the prepared compounds have potent activity against *B.subtilis* as compared to standard drug Ampicillin (**Table 3, Fig. 7**), but best activity was recorded of ligand **(2)** (MIC- 25 µM/ml). All the complexes showed almost similar activity against *S.pneumoniae*, but Cr(II) and Zn(II) complexes are most active (MIC ~ 36 µM/ml). A weak to excellent activity was exhibited by all compounds against *S.aureus* whereas Cr(II) complex showed excellent activity. The Co(II) complex showed maximum activity against the growth of *B.cereus* (**Table 4**), where moderate activity was observed of other compounds. The antibacterial activities of all the compounds are very much interesting and may lead as multi target drug.

Table 3. Zone of inhibition of HIMB ligand **(2)** and their metal ion complexes against selected bacterial species

Compounds	Bacterial zone of inhibition, in mm				Fungal zone of inhibition, in mm			
	B.subtilis	*S.aureus*	*B.cereus*	*S.pneumoniae*	*T.longifusus*	*C.albican*	*A.flavus*	*P.carinii*
HIMB	20	16	14	25	15	20	-	26
HIMBZn	18	11	20	28	-	12	19	16
HIMBCo	15	23	16	30	30	28	27	13
HIMBCr	15	26	19	29	23	-	-	10
Miconazole	-	-	-	-	10	23	26	30
Ampicillin	29	22	28	25	-	-	-	-

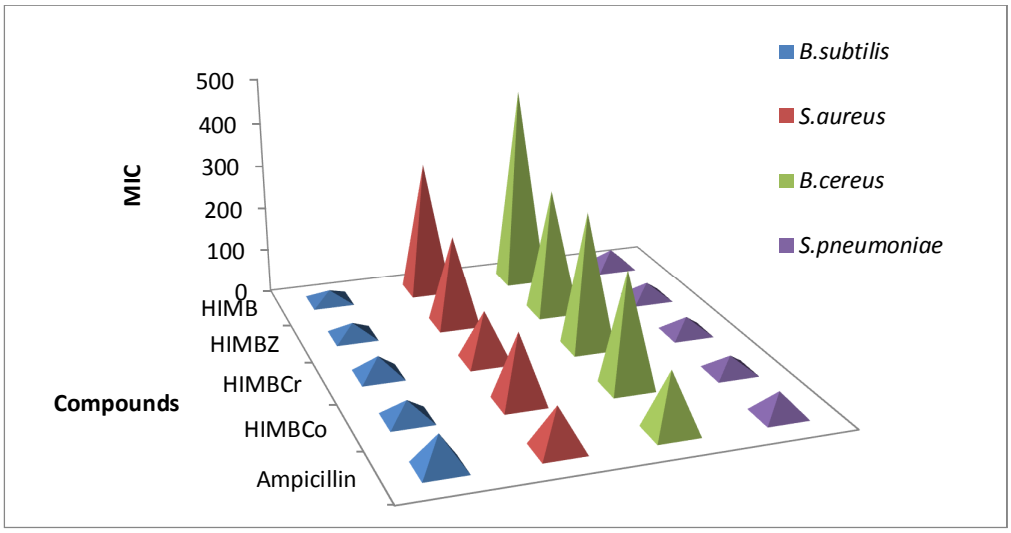

Fig. 7. Minimum inhibitory concentration of HIMB ligand **(2)** and their metal ion complexes against selected bacterial strain.

Table 4. Minimum inhibitory concentration of HIMB ligand **(2)** and their metal ion complexes against selected bacterial species

Compounds	MIC (µM/ml)			
	B.subtilis	*S.aureus*	*B.cereus*	*S.pneumoniae*
HIMB	25	300	450	42
HIMBZn	30	200	280	36
HIMBCr	42	110	300	36
HIMBCo	40	150	250	35
Ampicillin	70	90	128	50

2.2.4. In vitro study of cell viability

To test the toxicity of our compounds against the peripheral blood mononuclear cells, we chose only ligand (2) and Zn(II) which are most active against RT. We prepared 50-500 nM concentration of ligand **(2)** and Zn(II) complex and tested their toxicity by cell viability test using MTT. We observed that ligand **(2)** was toxic above 500 nM and Zn(II) complex was toxic above 350 nM. The % cell viability at different concentration is shown in the **Table 5**, delaviridine was used as control. It was concluded that both compounds do not show toxicity to the immune system at low concentration only toxic at higher concentration.

Table 5. Percentage viability test of HIMB ligand **(2)** and their Zn(II) complex on peripheral blood mononuclear cells.

	% Viability of PBMC		
Concentration (nM)	**HIMB**	**HIMBZn**	**Control**
50	101	96	100
100	99	98	98
250	96	110	95
350	101	60	100
400	105	10	105
500	70	0	99
550	30	0	98

Control-Delaviridine; PBMC-Peripheral blood mononuclear cell

2.2.5. Reverse transcriptase inhibition assay

Reverse transcriptase is an important enzyme of HIV cell to help in synthesis of genetic materials. We have synthesized Cr(II), Co(II) and Zn(II) complexes of N-hydroxy-4-[(hydroxyimino)methyl]benzamidine and studies their activity on reverse transcriptase using enzyme assay technique. The results were compared with those of standard drugs delaviridine. The percentage inhibition and inhibitory concentration at 50% (IC_{50}) of all compounds were observed and tabulated. The ligand **(2)** and Zn(II) complex showed the moderate activity (**Table 6, Fig. 8**), but Cr(II) and Co(II) complexes exhibited no activity against reverse transcriptase. HIMB ligand (2) displayed 45% inhibition at IC50 ~ 450 nM and Zn(II) complex can inhibit the growth up to 53% at IC50 ~ 250 nM. The observation shows the hydrogen bond donor and acceptor properties of ligand (2) and Zn(II) complex. The amidine moiety, distal hydroxyl group and coordination to Zn(II) metal ion is responsible for activity of ligand **(2)** and Zn(II) complex.

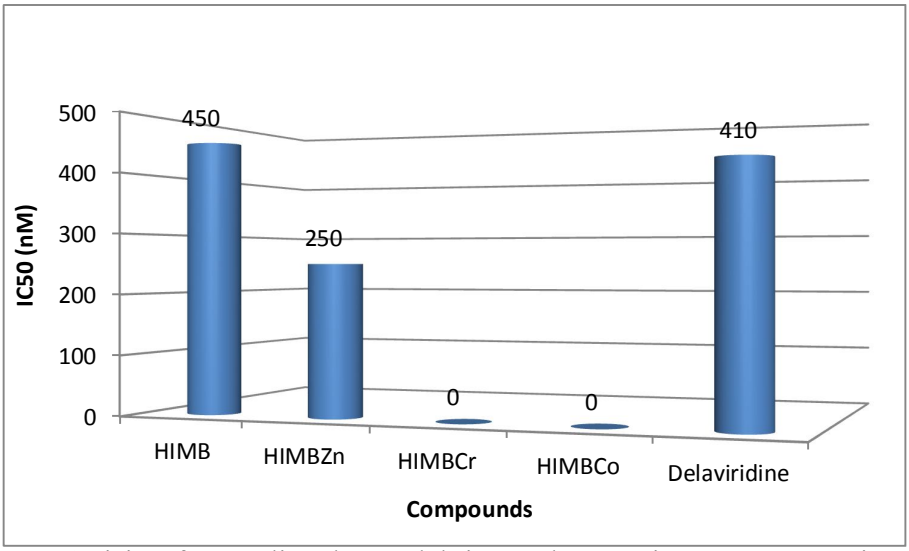

Fig. 8. Activity of HIMB ligand **(2)** and their complexes against reverse transcriptase

Table 6. Inhibition of reverse transcriptase from HIV-1 using HIMB ligand **(2)** and their complexes

Compounds	**% Inhibition**	**IC_{50} (nM)**
HIMB	45	450
HIMBZn	53	250
HIMBCr	-	-
HIMBCo	-	-
Delaviridine	68	410

The physicochemical data of ligand **(2)** displayed good solubility and OH-NH interaction to amino acid residues support inhibitory activity of ligand **(2)**.

The tetrahedral geometry of Zn(II) complex allows higher number of hydrogen bonding in the active site of RT increases their inhibitory activity. Another factor responsible for activity of Zn(II) complex against reverse transcriptase is their hydrophilicity and good solubility. It was studied that the higher permeability and hydrogen bonding increases their potencies. The present results show that ligand **(2)** and Zn(II) complex may be further studied increase their potencies for the future to control HIV-1. The Co(II) and Cr(II) complexes were studied and found as inactive against Reverse Transcriptase, although the activity was related to metal toxicity. These results were confirmed by separate studies of ligand, metal ions and metal complexes. The octahedral geometry and steric hindrance of Cr(II) and Co(II) complexes restricts approaching to the active site of RT so the activity diminished, the only inhibition was observed by preparing separate metal ion solutions which showed the metal toxicity.

3. Conclusions

The biological properties of N-hydroxy-4-[(hydroxyimino)methyl]benzamidine and its Zn(II), Co(II) and Cr(II) complexes showed good activity against selected fungal and bacterial species, also DNA cleavage activity. The possible tautomeric analogues of HIMB ligand **(2)** and tetrahedral geometry of Zn(II) complex furnish enhanced antimicrobial activity against *B.subtilis* and *S.aureus* . The ligand **(2)** and their Zn(II) complex were found more active against reverse transcriptase with the same reason as the antimicrobial activity. The highest activity of Co(II) and Cr(II) complexes were found against *B.subtilis*, *B.cereus* and *P.carinii* incorporated with higher permeability from cell wall of microbes. The solubility and steric factor is involved in RT inhibitory activity, considering this phenomenon may lead, we assume that HIMB ligand **(2)** and Zn(II) complex on proper study may lead as active anti HIV-1 as well as antimicrobial agents.

Acknowledgements

We are thankful to University Grant Commission, New Delhi, India, for providing Senior Research Fellow to meet our financial requirement. We are also thankful to The, Principal Moolji Jaitha College, Jalgaon (M.H.) for providing spectral analysis facility at their laboratory. Also grateful to IISER, Bhopal for providing sample analysis facility using NMR.

4. Experimental

4.1. Materials and methods

All the compounds were prepared and purified using AR grade reagents using the below mentioned procedures.

*4.2. Synthesis of ligand **(2)** and its metal(II) complexes*

*4.2.1. Synthesis of N-hydroxy-4-[(hydroxyimino)methyl]benzamidine ligand (HIMB) **(2)***

N-hydroxy-4-[(hydroxyimino)methyl]benzamidine was synthesized **(Scheme 1)** using known procedure reported elsewhere[18]. In a 250 ml conical flask, 4-[(hydroxyimino)methyl]benzonitrile, 2 g (0.012 mole), $NH_2OH.HCl$, 1.39 g (0.2 mole) and $NaNO_3$ 1.02 g (0.012 mole) was mixed, 80 ml water/ ethanol (2:1) was added to this mixture and stirred using magnetic stirrer followed by reflux for 2.5 hr. After completion of reaction solution was cooled to room temperature, crystals of N-hydroxy-4-[(hydroxyimino)methyl]benzamidine were separated out. Solvent was removed under reduced pressure, recrystallized using ethanol and followed by diethyl ether. Thin layer chromatography was used to check the purity.

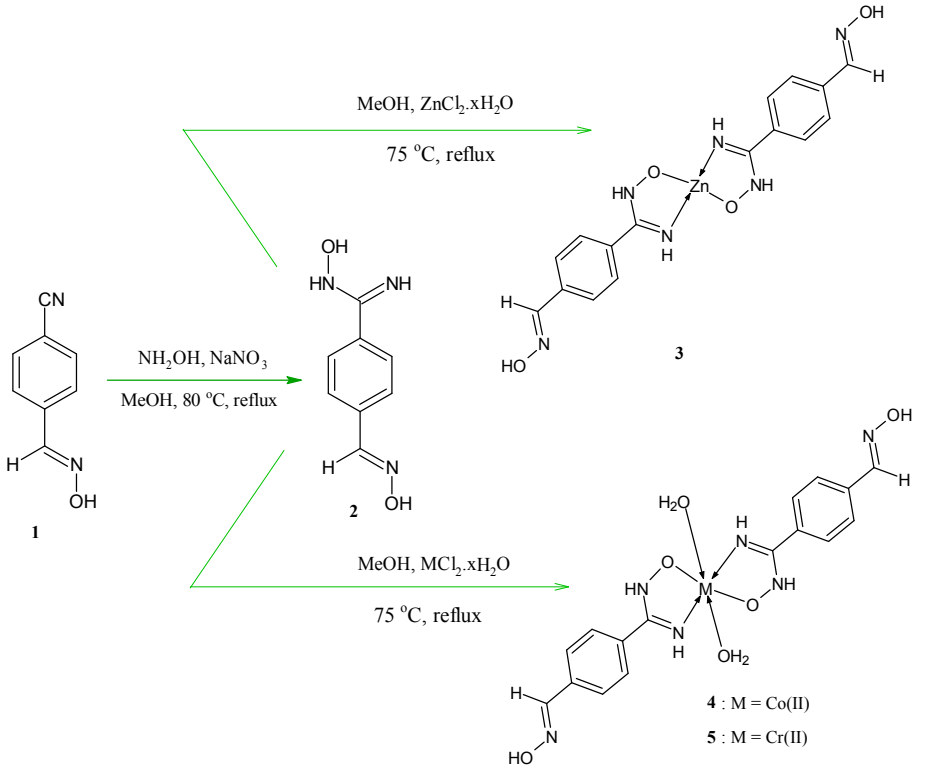

Scheme 1. Synthesis of N-hydroxy-4-[(hydroxyimino)methyl]benzamidine ligand **(2)** and its metal(II) complexes **(3-5)**.

4.2.2. Synthesis of N-hydroxy-4-[(hydroxyimino)methyl]benzamidine metal(II) complexes

Metal complexes were prepared by mixing methanolic solution of ligand **(2)** and metal salt in 1:2 (L:M) ratio. Ligand **(2)** was taken in 250 ml conical flask and metal salt were added drop wise using magnetic stirrer. The final solution was then transferred into a 250 ml round bottom flask and refluxed for 2 hr using water bath. Solution was cooled at room temperature, crystals of metal complexes were separated, filtered and recrystallized using ethanol, dried under vacuum.

4.3 Physical and Spectral Data

*4.3.1. N-hydroxy-4-[(hydroxyimino)methyl]benzamidine (HIMB) ligand **(2)***

Yield: 75%; Color: (white powder); m.p.: 93 °C; UV-Vis λ_{max}: 370 nm; ^{1}H NMR (DMSO-d_6, 400 MHz, ppm) δ: 10.93 (distal N-OH), 9.88 (amidine N-OH)5.99 (C=NH amidine), 7.39, 7.42, 7.44, 7.47 (Ar-H), 7.82 (H-C=N); ^{13}C NMR (DMSO-d_6, d, ppm): 128.78 (C1, C5), 153.10 (C7 amidine), 130.72(C4), 132.15(C3), 149.34(C7), 130.24, 130.72 (C2, C6); IR (KBr, cm^{-1}): 1653 (C=N), 972 (N-O), 1540 (C-N), 3292 (O-H), 3495 (distal OH); Mass (m/z): 179.06 $[C8H9N3O2]^{+}$; Anal. Calcd. For: C8H9N3O2 (179.17): C (53.63%), H (5.06%), N (23.45%), O (17.86%).

*4.3.2. N-hydroxy-4-[(hydroxyimino)methyl]benzamidine Zn(II) complex (HIMBZn) **(3)***

Yield: 65%; Color: (yellowish powder); m.p.: 165 °C; UV-Vis λ_{max}: 420 nm; ^{1}H NMR (DMSO-d_6, 400 MHz, ppm) δ: 10.91 (distal N-OH), 1.48 (C=NH amidine), 7.90, 7.92, 8.07, 8.29 (Ar-H), 8.25 (H-C=N); ^{13}C NMR (DMSO-d_6, d, ppm): 128.91 (C11, C15), 149.30 (C22 distal), 152.99(amidine C3), 129.60(C10), 130.74(C12, C13, C14); IR (KBr, cm^{-1}): 1660 (C=N), 1024 (N-O), 1610 (C-N), 543 (M-O), 511 (M-N), 3010 (distal OH); Mass (m/z): 420.05 $[C16H16N6O4Zn]^{+}$; Anal. Calcd. For: C16H16N6O4Zn (421.74): C (45.57%), H (3.82%), N (19.93%), O (15.17%), Zn (15.51%).

4.3.3. N-hydroxy-4-[(hydroxyimino)methyl]benzamidine Co(II) complex (HIMBCo) ***(4)***

Yield: 75%; Color: (dark brown). m.p.: 183 ºC; UV-vis (EtOH) λ_{max}: 520 nm(1.96); ^{1}H NMR (DMSO-d_6, 400 MHz, ppm) δ: 10.93 (distal N-OH), 1.50 (C=NH amidine), 7.90, 7.92, 8.07, 8.29 (Ar-H), 8.29 (H-C=N); ^{13}C NMR (DMSO-d_6, d, ppm): 128.91 (C11, C15), 161.09 (C3 amidine), 130.49(C13), 130.62(C12, 14), 149.34(C24); IR (KBr, cm^{-1}): 1648 (C=N), 993 (N-O), 2700 (C-N), 520 (M-O), 570 (M-N), 3344 (distal OH); Mass (m/z): 451.11 $[C16H20N6O6Co]^{+}$; Anal. Calcd. For: C16H20N6O6Co (451.29): C (42.58%), H (4.47%), N (18.62%), O (21.27%), Co (13.06%).

4.3.4. N-hydroxy-4-[(hydroxyimino)methyl]benzamidine Cr(II) complex (HIMBCr) ***(5)***

Yield: 57%; Color: (Dark green); m.p.: 178 ºC; UV-Vis λ_{max}: 510 nm (1.18); ^{1}H NMR (DMSO-d_6, 400 MHz, ppm) δ: 10.93 (distal N-OH), 1.50 (C=NH amidine), 7.90, 7.92, 8.07, 8.29 (Ar-H), 8.29 (H-C=N); ^{13}C NMR (DMSO-d_6, d, ppm): 128.91 (C11, C15), 161.09 (C3 amidine), 130.49(C13), 130.62(C12, 14), 149.34(C24); IR (KBr, cm^{-1}): 1665 (C=N), 1010 (N-O), 2710 (C-N), 530 (M-O), 580 (M-N), 3340 (distal OH); Mass (m/z): 444.08 $[C16H20N6O6Cr]^{+}$; Anal. Calcd. For: C16H20N6O6Cr (444.36): C (43.25%), H (4.54%), N (18.91%), O (21.06%), Cr (11.70%).

4.4. Biological evaluation

4.4.1. Antimicrobial activity

4.4.1.1. In vitro antibacterial activity

In this research work antibacterial activity of the Cr(II), Co(II) and Zn(II) metal complexes derived from N-hydroxy-4-[(hydroxyimino)methyl]benzamidine were evaluated in vitro against the four bacterial species *viz. E. coli, S.aureus, B.cereus and S.pneumoniae*, according to the literature protocol[20]. Filter paper disc method was used in this study at various concentrations, of test compounds in nutrient agar as medium. Sterilized filter papers of 30 mm diameter were soaked in solutions of different concentrations of ligand (2) and their metal complexes containing bacterial culture plates. These plates were incubated for 24 hr. at 35±0.5ºC. The zone of inhibition and minimum inhibitory concentration were measured and recorded. The obtained results were compared with those of standard drug imipenem.

4.4.1.2. In vitro antifungal activity

The antifungal efficacy of the prepared compounds was tested against *T.longifusus, C.albican, A.flavus and P.carinii* fungal species using the protocol mentioned in the literature[21]. All fungi were cultured in agar medium and incubated at 36ºC for 48 hr. The incubation chamber was kept humid. At the end of the incubation period, minimum inhibitory concentration (MIC) and zone of inhibition of all compounds against fungal species were recorded. Results were compared with the standard drug miconazole.

4.4.2. DNA cleavage activity

Ligand (2) and its metal complexes were studied to evaluate their nucleage activity of DNA using agarose gel electrophoresis[22]. Experiment was initiated by incubation of the solution containing 30 µM CT-DNA, 50-70 µM test samples and 50 µM hydrogen peroxide (H_2O_2) in Tris–HCl/NaCl buffer (pH 7.2) at 37ºC for 2 hr. After incubation, the solutions were electrophoresed for 2 hr. at 50V on 1% agarose gel in Tris–acetic acid–EDTA buffer (pH 7.2); ethidium bromide 1 µg cm^{-3} was used as staining agent. DNA cleavage activity of all compounds was measured using documentation chamber[23].

4.4.3. Cell viability test

Cell viability test of active compounds (HIMB and Zn(II) complex) on uninfected peripheral blood mononuclear cells were performed by MTT assay. Blood cells were taken in 80 wells plates and compounds were added in the concentration range of 50-500 nM. Culture was maintained at 37ºC under

5% CO_2 for 10 days. An aliquot of 30 µl MTT solution was added to it and the plated were read after 24 hr. Viable tissue produces formazan crystals which are solubilized with methanol according to the procedure reported elsewhere[24,25]. Tissue viability was determined by dividing the optical density at 570 nm of the formazan product.

4.4.4. In vitro reverse transcriptase inhibition assay

To test the reverse transcriptase inhibition activity of HIMB ligand **(2)** and their mortal complexes RT inhibition assay was used. A solution containing 50 µl (0.2 U) RT, 50 µl reaction mixture [primer, oligo (dT)15), biotin-dUTP, dTTP, tris–HCl buffer 50 mM (pH 7.8)], 20 µl ligand **(2)** and their metal complexes (150-1000 µM) were incubated for 1 hr. at 37ºC. The samples were then transferred to wells containing delaviridine drug plates and incubated at 37ºC for 1 hr. The plates were washed three times with buffer solution and 100 µl of anti-DIG-POD (peroxidase) [antibody to DIG (digoxigenin) conjugated to peroxidase] solution and incubated for further 1 hr. at 37ºC[26]. A substrate solution was prepared by AEBTSA (2,2'-azino-bis-(3-ethylbenzthiazoline-6-sulfonic acid and 200 µl of this solution was transferred into all wells of the plate, followed by incubation at 25ºC for 15 minutes. The reaction progress and completion was confirmed by the color development, which is different for all compounds. Control samples containing enzyme, reaction mixture only, and a known inhibitor of RT was run sidewise. The plates were by ELISA reader and intensity was measured via spectrophotometer at 405 nm. Percentage inhibition was calculated by the color developed for each compound based on the formula:

% inhibition= 100 x [(Test reagent absorbance/positive control absorbance) x 100)].

References

1. Global update on HIV treatment (2013) Results, impact and opportunities.
2. Bellucci L., Angeli L., Tafi A., Radi M., and Botta M. (2013) Unconventional Plasticity of HIV-1 Reverse Transcriptase: How Inhibitors Could Open a Connection "Gate" between Allosteric and Catalytic Sites. *J. Chem. Inf. Model.,* 53, 3117–3122.
3. Iyidogan P., Sullivan T. J., Chordia M. D., Frey K. M., and Anderson K. S. (2013) Design, Synthesis, and Antiviral Evaluation of Chimeric Inhibitors of HIV Reverse Transcriptase. *ACS Med. Chem. Lett.,* 4, 1183–1188.
4. Hua R., Doucet, J.P., Delamar, M., and Zhang, R. (2009) QSAR models for 2-amino-6-arylsulfonylbenzonitriles and congeners HIV-1reverse transcriptase inhibitors based on linear and nonlinear regression methods. *Eur. J. Med. Chem.,* 44, 2158–2171.
5. Reeves J.D., and Doms R.W. (2002) Human immunodeficiency virus type 2. *J. Gen. Virol.,* 83, 1253–1265.
6. Clercq E. D. (2002) New anti-HIV agents and targets. *Med. Res. Rev.,* 22, 531–565.
7. Telesnitsky A., and Goff S.P. (1997) Reverse transcriptase and the generation of retroviral DNA, in: *Retroviruses, Cold Spring Harbor Laboratory Press*, 121-160.
8. Nikolenko G.N., Palmer S., Maldarelli F., Mellors J.W., Coffin J.M., and Pathak V.K. (2005) Mechanism for nucleoside analog-mediated abrogation of HIV-1 replication: balance between RNase H activity and nucleotide excision. *Proc. Natl. Acad. Sci.* U. S. A., 102, 2093-2098.
9. Jochmans D. (2008) Novel HIV-1 reverse transcriptase inhibitors. *Virus Res.,* 134, 171-185.
10. Daisley R. W., and Shah V. K. (1984) Synthesis and antibacterial activity of some 5-Nitro-3-phenyliminoindol-2(3*H*)-ones and their *N*-mannich bases. *J. Pharm. Sci.,* 73, 407-408.
11. Mock C., Puscasu I., Rauterkus M.J., Tallen G., Wolff J.E.A., and Krebs B. (2001) Novel Pt(II) anticancer agents and their Pd(II) analogues: syntheses, crystal structures, reactions with nucleobases and cytotoxicities. *Inorg. Chim. Acta.,* 319 109–116.
12. Czapski G., and Goldstein S. (1991) Requirements for Sod Mimics Operating In Vitro to Work Also In Vivo. *Free. Radic. Res.*, 12, 167–171.

13. Sun R.W.-Y., Ma D.-L., Wong E.L.-M., and Che C.-M. (2007) Some uses of transition metal complexes as anti-cancer and anti-HIV agents. *Dalton Trans.,* 4884–4892.
14. Tepperman K., Zhang Y., Roy P.W., Floyd R., Zhao Z., Dorsey J.G., and Elder R.C. (1994) Transport of Dicyanogold (I) Anion. *Metal Based Drugs,* 1 433–443.
15. Wang B.L., Li Y.H., Wang J.G., Ma Y., and Li Z.M. (2004) Molecular design, synthesis and biological activities of amidine as new ketol-acid reductoisomerase inhibitors. *Bioorg. Med. Chem.,* 12, 5415-26.
16. Vicini P, and Zani F. (2005) Synthesis and antimicrobial activity of N-(1,2-benzisothiazol-3-yl)amidine. *Bioorg Med Chem.*, 13, 1587-97.
17. Marchenko N.B., Granik V.G., Glushkov R.G., Budanova L.I., Kuzovkin V.A., Parshin V.A., and Al'tshuler R.A. (1997) Synthesis and biological activity of N-(β-arylethyl)amidine and N,N′-bis(β-arylethyl)amidine. *Farmaco.*, 52, 21-24.
18. Raman N., Pothiraj K., and Baskaran T. (2011) DNA interaction, antimicrobial, electrochemical and spectroscopic studies of metal(II) complexes with tridentate heterocyclic Schiff base derived from 2′-methylacetoacetanilide. *J. Mol. Stru.,* 1000, 135-144.
19. Sheikh J., Juneja H., Ingle V., Ali P., and Hadda T.B. (2013) Synthesis and in vitro biology of Co(II), Ni(II), Cu(II) and Zn(II) complexes of functionalized beta-diketone bearing energy buried potential antibacterial and antiviral O,O Pharmacophore sites, *J. Sau. Chem. Soc.,* 17, 269-276.
20. Wolf G.H. and Shimer M.T. (1987) Polycyclic aromatic hydrocarbons physically intercalate into duplex regions of denatured DNA. *Biochem*. 26, 6392-6396.
21. Patil S.A., Naika V.H., Kulkarni A.D., and Badami P.S. (2010) DNA cleavage, antimicrobial, spectroscopic and fluorescence studies of Co(II), Ni(II) and Cu(II) complexes with SNO donor coumarin Schiff bases. *Spectrochim. Acta A.,* 75, 347–354.
22. Shiju C., Arish D., and Kumaresan S. (2013) Homodinuclear lanthanide complexes of phenylthiopropionic acid: Synthesis, characterization, cytotoxicity, DNA cleavage, and antimicrobial activity. *Spectro. Acta Part A: Mol. Biomol. Spectro.,* 105, 532-538.
23. Khoo T.J., Break M. K. B., Crouse, K.A., Tahir, M. I. M., Ali, A.M., Cowley, A.R., Watkin, D.J., and Tarafder, M.T.H. (2014) Synthesis, characterization and biological activity of two Schiff base ligand (2)s and their nickel(II), copper(II), zinc(II) and cadmium(II) complexes derived from *S*-4-picolyldithiocarbazate and X-ray crystal structure of cadmium(II) complex derived from pyridine-2-carboxaldehyde. *Inorg. Chim. Acta*., 413,68-76.
24. Pascaline N. F., Frankline K. K., Debra M., Ilia A. G., and James D. (2009) Tetra-chloro-(bis-(3,5-dimethylpyrazolyl)methane)gold(III) chloride: An HIV-1reverse transcriptase and protease inhibitor. *J. Inorg. Biochem.* 103, 190-194.
25. Yang S., Pannecouque C., Daelemans D., Ma X. D., Liu Y., Chen Fen-Er, and Clercq E. D. (2013). Molecular design, synthesis and biological evaluation of BP-*O*-DAPY and *O*-DAPY derivatives as non-nucleoside HIV-1 reverse transcriptase inhibitors. *European J. Med. Chem.,* 65, 134-143.
26. Wang J., Liang H., Bacheler L., Wu H., Deriziotis K., Demeter L. M., and Dykes C. (2010). The non-nucleoside reverse transcriptase inhibitor efavirenz stimulates replication of human immunodeficiency virus type 1 harboring certain non-nucleoside resistance mutations. *Viro.,* 402, 228-237.
27. Lautre H.K., Patil K., Youssouffi H., Hadda T.B., Bhatia V., and Pillai A.K. (2014) Synthesis and biological evaluation of purine nucleoside phosphorylase inhibitors from *P. falciparum. World J Pharma Pharmaceut. Sci.,* 3, 1053-1068.
28. Lautre H.K., Pandey S., Patil K., and Pillai A.K. (2013) 3-amino-n-hydroxybenzamidine and their transition metal complexes: synthesis and evaluation as thymidylate kinase inhibitors of *M.tuberculosis*. *Internat. J. Multidisci. Res.,* 2, 65-69.